

## Abstract

Magnetite nanoparticles (MNP) were synthesized and stabilized with carboxylated compounds citric acid – CA, poly(acrylic acid) – PAA, poly(acrylic acid-co-maleic acid) – PAM, humic acid – HA and gallic acid – GA (polymerizing *in situ* on the surface). Adsorption isotherms and bonding feature were determined and used to explain the changes in charge and aggregation states and salt tolerance of the MNPs. The thicker layer of macromolecular acids PAA, PAM and HA provides better stability at physiological pH and salt concentration compared to the CA and GA coatings. In addition, Fe(III)-CA complexation promotes the dissolution of the nanoparticles. The biocompatibility of the polyacid-coated MNPs was tested in cell proliferation experiments.

## Keywords

Carboxylated magnetite nanoparticles · small and macromolecular organic polyacids · adsorption · nanoparticle stabilization · overcharging · biocompatibility

Etelka Tombác e-mail: [tombacz@chem.u-szeged.hu](mailto:tombacz@chem.u-szeged.hu)

Márta Szekeres e-mail: [szekeres@chem.u-szeged.hu](mailto:szekeres@chem.u-szeged.hu)

Ildikó Y. Tóth

Dániel Nesztor

Erzsébet Illés

Department of Physical Chemistry and Materials Science,  
University of Szeged, Hungary

Angéla Hajdú

Rita Andrea Bauer

Department of Physical Chemistry and Materials Science,  
University of Szeged, Hungary

Laboratory of Nanochemistry, Semmelweis University, Budapest, Hungary

István Zupkó

Department of Pharmacodynamics and Biopharmacy, University of Szeged, Hungary

Ladislau Vékás

Center of Fundamental and Advanced Technical Research, RA-TD,  
Timisoara, Romania

## 1 Introduction

Magnetite nanoparticles (MNPs) are superparamagnetic iron oxide nanoparticles (also called SPIONs) that have been applied efficiently in a number of various biomedical applications such as MRI contrasting, targeted drug delivery and hyperthermia as discussed recently in a review paper [1]. In biomedicine, aqueous dispersions of MNPs (water based magnetic fluids, MFs) are required in general; the dispersion is achieved mainly by coating the particles with different organic compounds (e.g., dextrane, citric acid or oleic acid). Appropriate functional groups (e.g., carboxyl, amine, hydroxyl, mercapto, phosphate) of organic molecules are able to anchor organic molecules chemically on iron oxide surface via complex formation between  $\equiv\text{Fe}-\text{OH}$  sites and organic ligands [2]. The colloidal stability of MFs under physiological conditions (blood pH~7.2–7.4 and salt concentration ~0.15 M) and in high magnetic field gradient is of crucial importance. Most of these applications require the magnetic nanoparticles to be non-toxic, chemically stable, uniform in size, and well-dispersed in aqueous media [1,2].

The magnetite nanoparticles synthesized in Szeged have been stabilized with different carboxylated compounds [3,4]. The chemical interactions between the  $\equiv\text{Fe}-\text{OH}$  sites and the adsorbed carboxylic groups are specific, and so their bond strengths differ significantly from each other. Their stabilizing efficiency changes definitely due to the different structure and thickness of the coating layers on the MNPs, i.e., the different composition of the aqueous interface at the particle surface. Exceeding adsorption saturation, the nanoparticles become stabilized in a way of combined steric and electrostatic effects. It has been demonstrated that neither steric nor electrostatic effects alone provide sufficient stability under physiological conditions. Some of our products have been tested in MRI as contrast agents and in cell experiments *in vitro* [5,6]. The interaction of these carboxylated MFs with human plasma has been also studied within the framework of ESF network program EpiTopmap in Dublin, the results of which have been published recently [7].

In this paper we show how the pH sensitivity of amphoteric magnetite can be eliminated and how the colloidal stability of iron oxide nanomagnets can be enhanced via carboxylated layer formation on magnetic cores by using different organic polyacids.

## 2 Experimental

### 2.1 Materials

Magnetite ( $\text{Fe}_3\text{O}_4$ ) nanoparticles (MNPs) were synthesised from the mixture of  $\text{FeCl}_2$  and  $\text{FeCl}_3$  salts, according to the alkaline hydrolysis method [8–11]. The size of the resulting particles was determined on the basis of transmission electron microscopic pictures as d~8–10 nm (d is the mean particle diameter).

Citric acid (CA), gallic acid (GA), polyacrylic acid (PAA, Mw=1800 Da) and poly(acrylic-co-maleic) acid (PAM, Mw=3000 Da, 50 wt.% in  $\text{H}_2\text{O}$ ) were purchased from Sigma–Aldrich. Humic acid (HA) was extracted from peat (Keszthely, Hungary) with 0.1 M NaOH using the traditional alkaline procedure. The ash content of raw HA was lowered to < 1% treating with HF/HCl. The dried product was dissolved in NaOH solution, the amount of which was equivalent to the total acidity of HA determined separately [12] by potentiometric acid–base titration. The amount of humic acids in the experiments is given as the number of moles of carboxyl and phenolic OH groups in one gram of HA. The primary reason for this is that the latter functional groups participate in surface complexation reactions of the adsorption and thus control the reactivity of HA. In addition, because of their polydisperse and fractal nature [13] the molecular weight of these natural materials is undefined, so it cannot be used for HA quantification. The whole amount of the acidic groups related to the unit mass of HA, i.e., the total acidity (4.3 mmol/g), was used to give the concentration of HA solutions in mmol/L unit. The amounts of PAA and PAM are expressed through the number of carboxylic groups in the monomer units:

$$-\text{COOH}/M_{w,AA} = 1/72 = 0.0139 \text{ mol/g and}$$

$$-\text{COOH}/M_{w,AM} = 3/188 = 0.0159 \text{ mol/g.}$$

The pH and ionic strength were set by solutions of NaCl, HCl and NaOH, analytical grade products of Reanal (Hungary). Milli-Q water was used. All experiments were performed at room temperature ( $25 \pm 1^\circ\text{C}$ ).

### 2.2 Experimental methods

#### 2.2.1 Adsorption

The adsorption isotherms of the polyacids were determined by the batch method at  $\text{pH}=6.5\pm 0.5$  (denoted as  $\text{pH}\sim 6.5$ ) and constant ionic strength, 0.01 M (set by NaCl). The magnetite suspensions of 1–20 g/L concentration were equilibrated with the series of polyacid solutions in closed test tubes for 24 h at room temperature, the highest polyacid concentration being 10 mmol/L. The pH was adjusted by adding small portions of

either NaOH or HCl solutions, and checked at the end of the adsorption time. The equilibrium concentrations of GA, HA, PAA and PAM were determined spectrophotometrically in a USB4000 spectrometer (Ocean Optics) and those of CA by cerimetric titration [14] using ferroin indicator. The absorbance of the supernatants at 260 nm (GA) and 450 nm (HA) or the difference in the absorbances at 223 and 250 nm (PAA and PAM) were determined after perfect separation of the solid particles by centrifuging at 13000 RPM for 1 hour. At higher polyacid concentrations, the separation was assisted by a permanent magnet and membrane filtration (0.22  $\mu\text{m}$  MILLEX-GP).

#### 2.2.2 FTIR-ATR measurements

FTIR-ATR spectra were recorded with a Bio-Rad Digilab Division FTS-65A/896 spectrometer (with DTGS detector), using a Harrick's Meridian Split Pea Diamond ATR accessory. The absorbance of the samples was measured in single reflection mode over the 400–4000  $\text{cm}^{-1}$  frequency range with resolution of 2  $\text{cm}^{-1}$ , accumulating 256 scans. Magnetite suspensions, polyacid solutions or suspensions of the polyacid-coated MNPs were dried on the crystal surface. For FTIR experiments, the specific amount of added polyacids (mmol/g MNP) was varied and corresponded to the added amounts at the plateau of the adsorption isotherms. The background spectra were measured on clean and dry diamond crystal.

#### 2.2.3 Electrophoretic mobility measurements

Electrophoretic mobilities of the pure (naked) and the polyacid-coated magnetite samples were measured in a NanoZS (Malvern, UK) apparatus at  $25\pm 0.1^\circ\text{C}$ , in disposable zeta cells (DTS 1060). The settings of the instrument were checked by using a standard latex sample (Malvern, UK), the zeta potential of which is given as  $\sim 55\pm 5$  mV. The measurements were performed under optimal scattering condition ( $\sim 10^5$  counts per seconds), applying either 0.05 or 0.1 g/L magnetite concentration depending on the aggregation state of the dispersions. In one series of experiments the pH was changed between  $\sim 3$  and  $\sim 10$  keeping the added amount of polyacids (per one gram of MNP) constant, and in another, the added amount of polyacids was varied at  $\text{pH}\sim 6$ . The experiments were performed at constant ionic strengths 0.005 M (CA), 0.002 M (HA) and 0.01 M (GA, PAA and PAM). The measurements were started after one hour equilibration time. Prior to measurement, ultrasonic agitation for 10 s was applied in order to ensure optimum dispersion of the samples.

#### 2.2.4 Particle sizing - dynamic light scattering (DLS)

The hydrodynamic diameter of the particles was measured in a NanoZS apparatus (Malvern, UK) with a He-Ne laser ( $\lambda = 633$  nm), operating in backscattering mode at an angle of  $173^\circ$ . The stock sol of magnetite particles was diluted with NaCl electrolyte to achieve 0.1 g/L solid content and constant

ionic strengths as given above. The pH of the systems was adjusted in the range of 3 to 10, directly before the measurement. The stabilizing effect of the adsorption of polyacids was investigated at different added amounts. All measurements were performed at a given kinetic state achieved by 10 s of ultrasonication followed by 110 s of relaxation. The average values of the hydrodynamic diameter ( $Z$ -average values,  $Z_{ave}$ ) were calculated from the 3<sup>rd</sup> order cumulant fits of the correlation functions.

### 2.2.5 Coagulation kinetic experiments

Salt tolerance of the stabilized magnetite nanoparticles was tested in coagulation kinetic measurements by using Zetasizer 4 (Malvern, UK) apparatus. NaCl concentration was changed gradually from 0 mM to 1000 mM at pH~6.5. The magnetite sol concentration was set to 0.0025 g/L in order to achieve optimum light scattering and particle diffusion conditions, and the size evolution of aggregates was followed in time. The coagulation rate was calculated from the slope of the kinetic curves as explained before [8]. The stability ratio ( $W$ ) was calculated from the initial slopes of kinetic curves belonging to the slow and fast coagulation ranges as given in literature [15,16,17]. To determine the onset of fast coagulation regime, at least three different NaCl concentrations were used within the range of instant coagulation. The critical coagulation concentration (CCC) was determined from the  $\log_{10} W$  vs.  $\log_{10} c_{NaCl}$  (NaCl concentration) function. In a typical experiment, changes in the hydrodynamic diameter were monitored for an hour with a time resolution of 2 minutes.

### 2.2.6 Cytotoxicity experiments

The antiproliferative capacities of the prepared MNPs have been determined in vitro utilizing human cell lines HeLa (cervix adenocarcinoma), MRC-5 (fetal lung fibroblast cell) and A431 (cancer cells isolated from skin) by MTT ([3-(4,5-dimethylthiazol-2-yl)-2,5-diphenyltetrazolium bromide]) cell viability assay [18,19]. The cells were purchased from ECACC (European Collection of Cell Cultures, Salisbury, UK) and cultivated in minimum essential medium supplemented with 10% fetal bovine serum, 1% non-essential amino acids and an antibiotic antimyotomic mixture. All media and supplements were obtained from Life Technologies (Paisley, UK). The cells were grown in a humidified atmosphere of 5% CO<sub>2</sub> at 37°C. Briefly, a limited number of human cells (5000/well) were seeded onto a 96-well microplate and attached to the bottom of the well overnight. On the second day of the procedure, the original medium was removed and 200  $\mu$ L of a new medium, containing the polyacid-covered magnetite in concentrations of 5, 20 or 100 mg/L, was added. After incubation for 72 h, the living cells were assayed by the addition of 20  $\mu$ L of 5 mg/mL MTT solution. MTT was converted by intact mitochondrial reductase and precipitated as blue crystals during a 4-hour contact period. The medium was

then removed, and the precipitated crystals were dissolved in 100  $\mu$ L of dimethyl sulfoxide during a 60-min period of shaking. Finally, the reduced MTT was assayed at 545 nm, using a microplate reader. All experiments were carried out in duplicate with five parallel wells and wells with untreated cells were utilized as controls. Cisplatin was used as reference compound. The calculations of the results were carried out by means of computer program GraphPad Prism 2.01 (GraphPad Software, San Diego, CA, USA).

## 3 Results and discussion

### 3.1 Adsorption of polyacids

The adsorption isotherms of the low and high molecular weight carboxylic acids are seen in Fig. 1. All the isotherms, with the exception of PAA, are of high affinity (H-type isotherms) and the affinity increases in the order CA ~ GA < PAM < HA. The adsorption of HA, PAA and PAM reaches definite plateau region at the adsorbed amounts of ~0.85, ~0.6 and ~0.9 mmol/g, respectively. On the contrary, after the high-affinity limit at ~0.1 mmol/g, the adsorption of both CA and GA continues without reaching a plateau value.

The linear increase in the adsorbed amounts is probably connected with the polymerization of the molecules in the adsorption layer. It is well known that GA polymerizes easily in solution [20], and polymerization of surface-bound GA continues at an even greater rate [21].

Besides considering the most common pH of biological liquids like blood, the solution conditions for adsorption, pH~6.5 and ionic strength 0.01 M, were chosen on the basis of the charging behaviour of the MNP and the polyacids [6,8,22] in order to provide optimal electrostatic attraction. However, additional specific interactions are needed for achieving

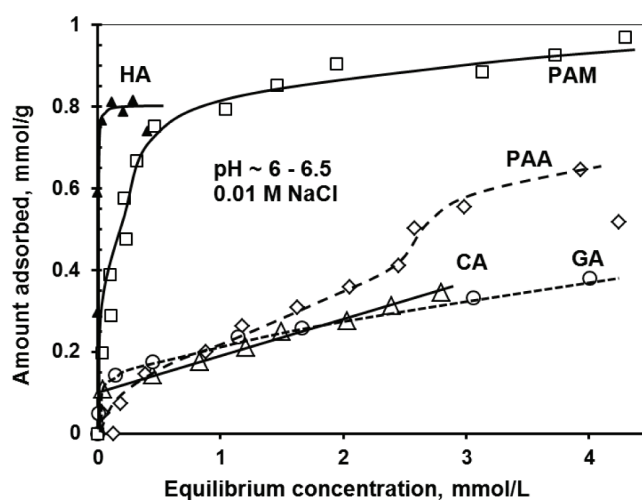
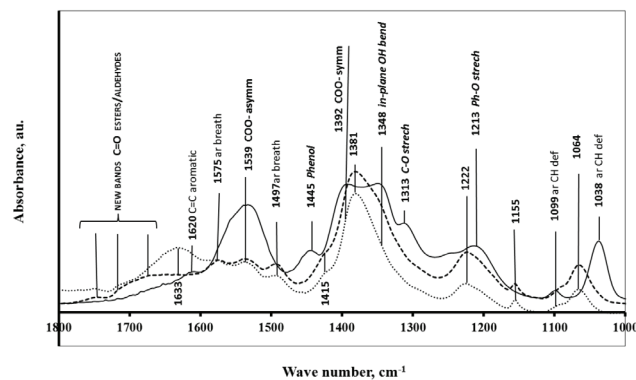


Fig. 1. Adsorption isotherms of carboxylic acids on magnetite nanoparticles measured at pH~6–6.5 and 0.01 M ionic strength. (The amount of the macromolecular polyacids (HA, PAA and PAM) was related to the moles of acidic groups.).

sufficient persistence of the coated MNPs under the conditions of biomedical application; i.e., high salt concentration, magnetic field and dilution during distribution in the blood and tissues. The specific interactions of the polyacids with MNP surface have been identified using FTIR-ATR measurements. The spectral changes of PAA and PAM due to adsorption are discussed in our recent publications [6,23]. Although detailed study of GA adsorption will be given in our subsequent publication, one series of FTIR spectra is presented in Fig. 2. In the case of HA adsorption, FTIR spectra could not be used, because the analysis is too complicated due to the overlaps of absorption bands of many different functional groups. The involvement of the carboxylic groups in the adsorption can be seen as the changes in the characteristic band frequencies of protonated carboxyl groups (C=O stretching band  $\nu_{\text{C=O}} \sim 1700 \text{ cm}^{-1}$  and C–OH stretching/bending vibration  $\nu_{\text{COH}} \sim 1200 - 1300 \text{ cm}^{-1}$ ) and deprotonated carboxylates (asymmetric and symmetric vibrations of  $\nu_{\text{COO}^-,\text{as}} \sim 1600 \text{ cm}^{-1}$  and  $\nu_{\text{COO}^-,\text{sym}} \sim 1400 \text{ cm}^{-1}$ , respectively). The results are collected in Table 1.

At pH~6.5, CA and GA are fully deprotonated, and so –C=O and –C–OH bands are absent from the spectra both before and after the adsorption. The degree of dissociation of PAA and PAM is ~0.6, and the protonated carboxyl groups are adsorbed in an H-bonding mechanism with the participation of the –C=O groups, as it is seen from the considerable shifts of 17 and 23  $\text{cm}^{-1}$ , respectively. The asymmetric and symmetric –COO<sup>-</sup> vibration frequencies of PAA do not shift, revealing no participation of this group in the adsorption, and thus the absence of inner sphere metal-carboxylate surface complex formation [6]. The latter complex, however, forms in the adsorption of CA and PAM, as it is seen from the considerable shifts in both the symmetric and asymmetric –COO<sup>-</sup> vibrations. The asymmetric and symmetric –COO<sup>-</sup> stretching frequencies of CA shifted from 1562 to 1620 and from 1387 to 1396  $\text{cm}^{-1}$ , respectively. In the spectra of adsorbed GA (Fig. 2), the asymmetric –COO<sup>-</sup> stretching frequency remains at 1539  $\text{cm}^{-1}$ , but its relative intensity decreases considerably due to adsorption. On the other hand, the symmetric stretching frequency changes to lower wave number (from 1392 to 1381  $\text{cm}^{-1}$ ), revealing that excitation of this vibration mode becomes easier in the adsorbed state as compared to that in the free state. To explain the latter observation, we should note that free GA is dried from solution on the surface of the ATR diamond crystal; thus the –COO<sup>-</sup> groups are supposedly better coordinated in the dried state than in the adsorbed state at the MNP surface. On the basis of the FTIR spectra we can state that the carboxylate group is not involved in GA adsorption. We have proven the formation of direct metal-carboxylate surface complexes in the case of CA, PAM and HA [12,14,22,23] and only H-bonding in the case of PAA [6], and concluded that surface Fe-carboxylate complex bonds can form only when the geometric arrangement of the neighbouring carboxyl groups matches the distance between



**Fig. 2.** FTIR-ATR spectra of GA (solid line), GA@MNP at 0.1 mmol/g (dotted line) and GA@MNP at 0.25 mmol/g (dashed line) added amount of GA; pH~6.5 and I=0.01 M. The bands corresponding to the specific structural elements are distinguished by typesetting: carboxylate – bold; phenolic – bold italic; aromatic ring – normal; esters (formed in surface catalysed polymerization) – capital.

**Tab. 1.** Frequency shifts of the carboxyl IR bands in the process of polyacid adsorption on magnetite nanoparticles at pH~6.5 and I=0.01 M.

Absorption bands (cm-1)	$\Delta\nu (\nu_{\text{adsorbed}} - \nu_{\text{free}}), \text{cm}^{-1}$				
	CA	GA	PAA [6]	PAM [23]	
-COOH	C=O stretching (~1700)	N/A	N/A	17	23
	C-OH stretching (~1280)	N/A	N/A	0	0
-COO <sup>-</sup>	asym stretching (~1600)	58	0	0	7
	sym stretching (~1400)	9	-11	0	4

$\equiv\text{Fe-OH}$  surface sites. We have found that carboxylic groups belonging to neighbouring carbon atoms in CA and in the carbon backbone of PAM and HA can take part in such interaction. The neighbouring carboxylates in PAA belong to every second C atom of the backbone of polyacid chain, which is geometrically unfavourable for Fe-carboxylate formation. The geometric fitting between the functional groups of the adsorbates and the surface sites of the adsorbents is frequently found to be determining for surface complex formation [24].

The high adsorption affinity of GA can result from complex bond formation of neighbouring phenolic OH groups with the  $\equiv\text{Fe-OH}$  sites [25], as well as from  $\pi$ -electron interactions with the polar surface of the MNPs. The FTIR spectra in Fig. 2 present evidence of the above two kinds of specific interactions. We discuss the changes in the frequency and intensity of the most characteristic bands belonging to the three specific parts of GA molecule (the carboxylate group, the aromatic ring and the phenolic OH groups) separately. In addition, new bands appearing in the spectra of GA@MNP were identified as belonging to esters or aldehydes. The bands related to the phenolic groups show a mixed behaviour.

The 1445  $\text{cm}^{-1}$  phenol vibration shifts to lower wave number 1415  $\text{cm}^{-1}$ , and the 1348  $\text{cm}^{-1}$  in-plane OH bending and the

1313  $\text{cm}^{-1}$  C-O stretching band either disappear or become shoulders at unchanged frequencies, showing that there are OH groups not participating in bonding. The 1213  $\text{cm}^{-1}$  phenolic Ph-O stretching, on the other hand, is shifted to 1222  $\text{cm}^{-1}$ , showing that there are also phenolic groups that undergo adsorption interaction. The mixed behaviour of the phenolic OH groups can be readily explained by that only two neighbouring of the three OH groups take part in the surface complex formation. It is worth noting that the geometric condition for surface complexation of the phenolic OHs is the same as discussed before for the carboxylates [6], namely that they belong to neighbouring carbon atoms. The aromatic ring of GA is represented by the 1620  $\text{cm}^{-1}$  band of C=C, shifted to 1633  $\text{cm}^{-1}$ , and by the 1099  $\text{cm}^{-1}$  and 1038  $\text{cm}^{-1}$  bands of aromatic CH deformation, shifted to 1155 and 1064  $\text{cm}^{-1}$ , respectively. All the three vibrations require more energy to excite in the adsorbed state, showing that the aromatic ring is firmly connected with the MNP surface, probably lying flat on it. There are two additional bands at frequencies of 1575 and 1497  $\text{cm}^{-1}$ , characteristic of the so called aromatic ring breathing [26] that do not change their position upon adsorption, but become resolvable in the spectra only after decreasing the intensity of the asymmetric stretching vibration of  $-\text{COO}^-$  at 1539  $\text{cm}^{-1}$ . The stretching and contraction of the ring is not influenced by the adsorption, which also supports the probability of lying GA molecules on the surface. Entirely new absorption bands appear in the GA@MNP spectra at the higher wave numbers of  $\sim 1660$ ,  $\sim 1720$  and  $\sim 1750$   $\text{cm}^{-1}$ , absent from the spectrum of free GA. These bands are most likely due to the formation of ester- or aldehyde linkages between two GA molecules in the adsorbed state. This finding supports the surface catalysed polymerization of GA found in case of adsorption at clay mineral surfaces [21].

### 3.2 Electrokinetic potential and particle size of polyacid-coated MNPs

The addition of all carboxylic acids to the MNP dispersions at pH $\sim$ 6.5 and I= 0.01 M had a very similar, pronounced effect on the electrokinetic potential of the particles, discussed to some extent in [27]. Shortly, the original positive charge of the MNPs is neutralized at  $\sim 0.15$  mmol/g of added amounts of all polyacids except for GA ( $\sim 0.05$  mmol/g). Thus, the isoelectric points (IEP) with respect to the added amounts of polyacids do not provide a clear distinction of the two separate adsorption mechanisms: (i) high-affinity adsorption due to ligand exchange reaction to form Fe-carboxylate surface complexes for PAM [23], HA and CA and (ii) the absence of high-affinity ligand exchange for PAA [6]. On the other hand, the presentation of electrokinetic potential data in the function of the adsorbed amounts of polyacids (Fig. 3) clearly differentiates these two mechanisms. The IEPs for the high-affinity, ligand exchange adsorption of HA, PAM and CA are found at  $\sim 0.15$  mmol/g of adsorbed amounts, while those of PAA

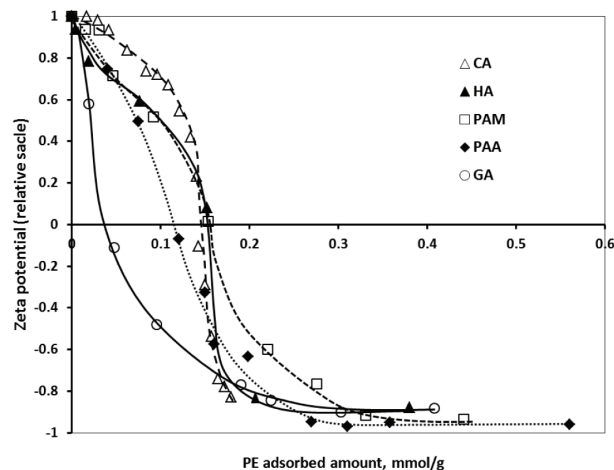


Fig. 3. Plots of the electrokinetic potential values of polyacid coated MNPs in function of the adsorbed amounts of polyacids HA, PAM, PAA, CA and GA, measured at pH  $\sim$ 6–6.5, and at I=0.01 M. (The amount of the macromolecular polyacids (HA, PAA and PAM) was related to the moles of their acidic groups. The error in the relative values of zeta potentials is  $\pm 0.1$ ).

and GA are at  $\sim 0.12$  and  $\sim 0.04$  mmol/g, respectively. Although GA is adsorbed with high-affinity as well, the immediate steep decrease in the zeta potential (and extremely low IEP) should be connected with surface polymerization (discussed in [23] and supported by FT-IR results in Fig. 2) proceeding in parallel with the adsorption. Further addition of polyacids leads to zeta potential reversal. The highest potential of the negatively charged surfaces is similar for all polyacid coatings, around  $-40$  mV. The relative scale for the zeta potential axis in Fig. 3 is used to eliminate the random deviations in the actual measured values of naked MNPs, caused by small variations in the experimental conditions (e.g., pH  $\sim$ 6.5; the standard error in zeta potentials is  $\pm 5$  mV).

The pH-dependent electrokinetic potential and hydrodynamic diameter of the different carboxylic acid-coated MNPs allows detecting the pH range, in which the coated nanoparticles are dispersed individually in a colloidal stable state. For biomedical application, the polyacid@MNP agents must be well dispersed in the environment of physiological pH ( $\sim 7$ ), where magnetite particles themselves would be fully aggregated because their point of zero charge is at pH=8.0 $\pm$ 0.1 [11]. Polyacid adsorption overcharges the MNP surface and by this, it lowers the pH of the isoelectric point of MNPs. The degree of IEP lowering depends on the adsorbed amount of polyacids. We have collected the IEP values of polyacid@MNPs at different added amounts of polyacids in Table 2, in parallel with the pH ranges, over which the particles undergo aggregation (seen as the increase in the hydrodynamic diameters,  $Z_{\text{ave}}$ , in the DLS measurements). The pH-dependent stability changes in parallel with IEP in each case, shifting the pH-range of aggregation to  $< 7$ . Differences appear only in the amounts that can completely mask the original amphoteric feature of magnetite.

In addition, small deviation in the average hydrodynamic sizes of particles covered by different organic acids has been found (data not shown), which is caused by the difference in the structure and thickness of the adsorbed layers. High molecular weight polyelectrolytes generally led to the higher values of hydrodynamic diameter, e.g., ~150 nm for HA, PAA and PAM, versus ~100 nm for CA and GA stabilized systems. The reason for this is that the macromolecular compounds form thick and well-structured coating layers. The monocarboxylic GA was able to shift the aggregation pH only to about ~5, meaning that the monomeric GA-coating is not sufficient to prevent particle aggregation at physiological pH.

### 3.3 Salt tolerance of the polyacid coated MNPs

Salt tolerance of the MNPs coated with different amounts of carboxylic acids was measured in coagulation kinetics experiments at pH~6.5. We have observed that the critical coagulation concentration (CCC) of NaCl increases with increasing amount of carboxylic acid, if the IEP of the actual carboxylic acid coated MNP is lower than pH~6.5. In case the added amount of carboxylic acids is insufficient to decrease the IEP well below pH~6.5, the CCC does not increase compared to that of the naked MNPs. At low coverage, the partially covered (i.e., decorated) particles can aggregate because of the electrostatic attraction between the oppositely charged uncoated and coated patches on the particle surfaces [8,28]. The highest attained values of CCC and the respective amounts of added polyacids are collected in Table 3. It is seen that the small molecules CA and GA cannot stabilize the MNPs at neutral pH to resist higher salt concentrations, despite the approximately identical values of electrokinetic potentials (around -40 mV at pH ~6.5, Fig. 3). On the contrary, the thicker coating shells prepared with macromolecular polyelectrolytes PAA, PAM, HA enhance the salt resistance equally up to CCC ~ 500 mM. CCC values for colloidal particles relevant to the magnetite/polyelectrolyte systems studied here are very rare in literature. Hu and co-workers [29] found that CCC of magnetite nanoparticles is 125.5 mM in the presence of 20 mg/g of humic acid at pH=9.8, which is only quarter of our highest attained values.

### 3.4 Biocompatibility of polyacid coated MNPs

For biomedical application it is inevitable that the polyacid-coated MNPs are biocompatible. We have tested the biocompatibility of MNPs with CA, GA, HA, PAA and PAM coatings. The results in Fig. 4 show that all inhibition percentages were smaller or at least not significantly higher than 25%, thus neither of the particles exhibited cytotoxic effect [18,19,30]. The highest inhibition was observed for the CA, HA and PAA coatings, while the effect of GA and PAM-coated particles was in principle negligible, with inhibition lower than 5%. The excellent biocompatibility of GA@MNPs explains the necessity

**Tab. 2.** Effect of the quality and added amounts of carboxylic acids on the IEP and the pH-range of aggregation of MNPs

Carboxylated coating agents	Added amount* mmol/g	pH of IEP	pH-range of aggregation
CA	0.13	6.0	4.5-9.5
	0.65	3.0	<4.5
GA	0.02	6.8	<9
	0.1	4.8	<7.5
	0.6	4.2	<6
	1.8	2.7	<5.2
PAA	0.1	6.5	4-7
	0.48	3.8	3.5-5.5
PAM	1.15	3.0	<3.5
	0.1	6.2	3.5-8.5
	0.47	3.5	<5
HA	1.3	2.5	<3.5
	0.08	7.2	4.5-8.5
	0.8	<3	<3

\* The added amount of HA, PAA and PAM was related to the moles of their acidic groups.

**Tab. 3.** CCC values of uncoated and polyacid coated MNPs, measured at pH~6.5.

Polyacids@MNP	Added amount* mmol/g	Approx. CCC NaCl, mM
Naked MNP	0	1
CA@MNP	0.3	70
GA@MNP	2	20**
PAA@MNP	1.12	500
PAM@MNP	1.18	500
HA@MNP	1.5	500

\* The added amount of HA, PAA and PAM was related to the moles of their acidic groups.

\*\* measured after 1 hour standing

of further experiments in the direction of increasing colloidal stability of GA-coated particles, which can be based on the surface catalysed polymerization of GA in the adsorbed state. Some indication can be found in literature regarding the insufficient biocompatibility of citrate-coated MNPs [31,32]. It is likely that some cell toxicity concerns lie behind stopping – at least for the moment – of the clinical trials of VSOP-C184, the only CA@MNP product tested up-to-date. The phase I clinical evaluation terminated in 2004 [33], yet there is no information about its continuation. In the case of the three other coating molecules, direct correlation is seen between the biocompatibility and the strength of polyacid adsorption. It is apparent that high-affinity adsorption (mainly due to the formation of direct metal-carboxylate and metal-OH complexes on the MNP surface) provided higher biocompatibility to the PAM and

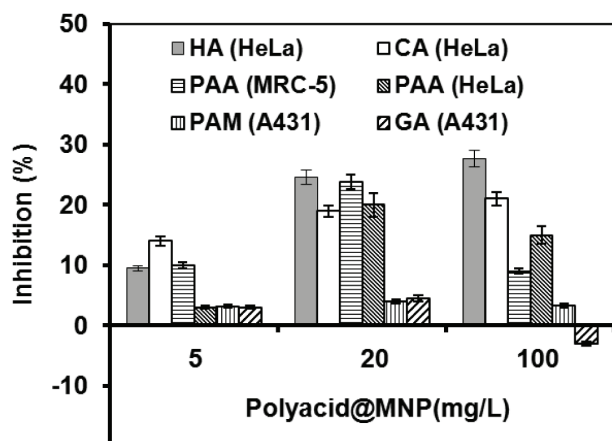


Fig. 4. Cell inhibition of the CA, GA, HA, PAA and PAM-coated MNPs, added in identical concentrations to human cell cultures HeLa, MRC-5 and A431. The error bars represent standard deviation, ranging in 5 to 10 %.

GA coated particles than the weaker adsorption of PAA (lacking the inner-sphere complexation ability) to the PAA-coated ones. A comparison of the effects of a polyacid@MNP on healthy and cancerous cells is seen in the examples of PAM@MNP incubated MCR-5 and HeLa cell lines. We can see that viability of both types of cells is affected similarly: at 5 and 20 mg/L healthy cells are somewhat more sensitive to the PAA@MNP addition, while at 100 mg/L concentration the opposite is observed.

#### 4 Conclusions

The adsorption of different organic acids and its effect on the pH-dependent colloidal stability and salt tolerance of

magnetite nanoparticles were studied. The adsorbed amounts were given in the molar amount of acidic groups per unit mass of iron oxide, which was useful especially for macromolecular acids HA, PAA and PAM. This approach makes the quantitative comparison of the adsorbed amounts of acidic groups of small or large organic acids (also the well- or undefined polyelectrolytes) with the amount of surface charge of magnetite practicable. Thus the charge neutralization and charge reversal can be interpreted on chemical basis. The specific chemical nature of the interacting partners has to be considered, because chemical reactions take place at electrified interfaces, i.e., the functional groups of organic acids interact with the charged/uncharged surface sites of magnetite. The exact feature of the specific interactions depends definitely on the geometry of complexing groups of organic molecules.

Trace amounts of the organic acids can destabilize magnetite dispersions, while their high loading masks the original surface properties of magnetite and improves colloidal stability and salt tolerance of dispersions. In the presence of greater amounts of polyacids (above the adsorption saturation), the surface coverage of magnetite becomes completed causing a sign reversal of particle charge and overcharging of nanoparticles. The thicker layer of the macromolecular coating shell of PAA, PAM or HA provides better electrosteric stability than that formed with the small molecules of CA or GA. Coagulation kinetics experiments test the salt tolerance of coated MNPs, i.e., their resistance against aggregation in physiological environment. Study of the adsorption mechanism of the polyacids at the MNP surface reveals that high-affinity adsorption through surface metal-carboxylate complexes is the prerequisite for optimal quality of coating (PAM@MNPs) [24] and for increased biocompatibility of MFs (PAM@MNPs and GA@MNPs).

#### Acknowledgements

This work was supported by OTKA (NK 84014) foundation and by TÁMOP-4.2.2.A-11/1/KONV-2012-0047 project.

#### References

- Amstad E., Textora M., Reimhult E., *Stabilization and functionalization of iron oxide nanoparticles for biomedical applications*. *Nanoscale*, 3(7), 2819–2843 (2011). DOI: [10.1039/C1NR10173K](https://doi.org/10.1039/C1NR10173K)
- Boyer C., Whittaker M. R., Bulmus V., Liu J., Davis T. P., *The design and utility of polymer-stabilized iron-oxide nanoparticles for nanomedicine applications*. *NPG Asia Materials*, 2(1), 23–30 (2010). DOI: [10.1038/asiamat.2010.6](https://doi.org/10.1038/asiamat.2010.6)
- Tombácz E., Bica D., Hajdú A., Illés E., Majzik A., Vékás L., *Surfactant double layer stabilized magnetic nanofluids for biomedical application*. *Journal of Physics: Condensed Matter*, 20(20), 204103 (2008). DOI: [10.1088/0953-8984/20/20/204103](https://doi.org/10.1088/0953-8984/20/20/204103)
- Hajdú A., Tombácz E., Illés E., Bica D., Vékás L., *Magnetite nanoparticles stabilized under physiological conditions for biomedical application*. *Progress in Colloid and Polymer Science*, 135, 29–37 (2008). DOI: [10.1007/2882\\_2008\\_111](https://doi.org/10.1007/2882_2008_111)
- Jedlovsky-Hajdú A., Tombácz E., Bányai I., Babos M., Palkó A., *Carboxylated magnetic nanoparticles as MRI contrast agents: Relaxation measurements at different field strengths*. *Journal of Magnetism and Magnetic Materials*, 324(19), 3173–3180 (2012). DOI: [10.1016/j.jmmm.2012.05.031](https://doi.org/10.1016/j.jmmm.2012.05.031)
- Hajdú A., Szekeres M., Tóth I. Y., Bauer R. A., Mihály J., Zupkó I., Tombácz E., *Enhanced stability of polyacrylate-coated magnetite nanoparticles in biorelevant media*. *Colloids and Surfaces B: Biointerfaces*, 94, 242–249 (2012). DOI: [10.1016/j.colsurfb.2012.01.042](https://doi.org/10.1016/j.colsurfb.2012.01.042)
- Jedlovsky-Hajdú A., Bombelli F. B., Monopoli M. P., Tombácz E., Dawson K. A., *Surface coatings shape the protein corona of SPIONs with relevance to their application in vivo*. *Langmuir*, 28(42), 14983–14991 (2012). DOI: [10.1021/la302446h](https://doi.org/10.1021/la302446h)

- 8 Illés E., Tombácz E., *The effect of humic acid adsorption on pH-dependent surface charging and aggregation of magnetite nanoparticles*. Journal of Colloid and Interface Science, 295(1), 115–123 (2006). DOI: [10.1016/j.jcis.2005.08.003](https://doi.org/10.1016/j.jcis.2005.08.003)
- 9 Vékás L., Bica D., Marinica O., *Magnetic nanofluids stabilized with various chain length surfactants*. Romanian Reports in Physics, 58(3), 257–267 (2006).
- 10 Bica D., Vékás L., Avdeev M. V., Marinica O., Socoliuc V., Balasoiu M., Garamus V. M., *Sterically stabilized water based magnetic fluids: synthesis, structure and properties*. Journal of Magnetism and Magnetic Materials, 311(1), 17–21 (2007). DOI: [10.1016/j.jmmm.2006.11.158](https://doi.org/10.1016/j.jmmm.2006.11.158)
- 11 Tombácz E., Illés E., Majzik A., Hajdú A., Rideg N., Szekeres M., *Ageing in the inorganic nanoworld: example of magnetite nanoparticles in aqueous medium*. Croatica Chemica Acta, 80(3–4), 503–515 (2007).
- 12 Illés E., Tombácz E., *The role of variable surface charge and surface complexation in the adsorption of humic acid on magnetite*. Colloids and Surfaces A: Physicochemical Engineering Aspects, 230(1–3), 99–109 (2003). DOI: [10.1016/j.colsurfa.2003.09.017](https://doi.org/10.1016/j.colsurfa.2003.09.017)
- 13 Tombácz E., *Colloidal properties of humic acids and spontaneous changes of their colloidal state under variable solution conditions*. Soil Science, 164(11), 814–824 (1999).
- 14 Binnemans K., *Applications of tetravalent cerium compounds*. in ‘Handbook on the Physics and Chemistry of Rare Earths’ (eds.: Gschneidner K. A., Bünzli J.-C. G., Pecharsky V. K.,) Elsevier B.V., Amsterdam, 36, 281–391 (2006).
- 15 Hunter R. J., *Foundations of Colloid Science: Vol. I*. Oxford University Press, Oxford, U. K. (1987).
- 16 Schudel M., Behrens S. H., Holthoff H., Kretzschmar R., Borkovec M., *Absolute aggregation rate constants of hematite particles in aqueous suspensions: a comparison of two different surface morphologies*. Journal of Colloid and Interface Science, 196(2), 241–253 (1997).
- 17 Kretzschmar R., Holthoff H., Sticher H., *Influence of pH and humic acid on coagulation kinetics of kaolinite: a dynamic light scattering study*. Journal of Colloid and Interface Science, 202(1), 95–103 (1998).
- 18 Gupta A. K., Curtis A. S. G., *Lactoferrin and ceruloplasmin derivatized superparamagnetic iron oxide nanoparticles for targeting cell surface receptors*. Biomaterials, 25(15), 3029–3040 (2004). DOI: [10.1016/j.biomaterials.2003.09.095](https://doi.org/10.1016/j.biomaterials.2003.09.095)
- 19 Mosmann T. J., *Rapid colorimetric assay for cellular growth and survival: application to proliferation and cytotoxicity assays*. Journal of Immunological Methods, 65(1–2), 55–63 (1983). DOI: [10.1016/0022-1759\(83\)90303-4](https://doi.org/10.1016/0022-1759(83)90303-4)
- 20 Giannakopoulos E., Drosos M., Deligiannakis Y., *A humic-acid-like polycondensate produced with no use of catalyst*. Journal of Colloid and Interface Science, 336(1), 59–66 (2009). DOI: [10.1016/j.jcis.2009.03.037](https://doi.org/10.1016/j.jcis.2009.03.037)
- 21 Tombácz E., Szekeres M., Baranyi L., Micheli E., *Surface modification of clay minerals by organic polyions*. Colloids and Surfaces A: Physicochemical Engineering Aspects, 141(3), 379–384 (1998). DOI: [10.1016/S0927-7757\(98\)00241-6](https://doi.org/10.1016/S0927-7757(98)00241-6)
- 22 Hajdú A., Illés E., Tombácz E., Borbáth I., *Surface charging, polyanionic coating and colloid stability of magnetite nanoparticles*. Colloids and Surfaces A: Physicochemical Engineering Aspects, 347(1–3), 104–108 (2009). DOI: [10.1016/j.colsurfa.2008.12.039](https://doi.org/10.1016/j.colsurfa.2008.12.039)
- 23 Tóth I. Y., Bauer R. A., Nesztor D., Szekeres M., Tombácz E., *Designed polyelectrolyte shell on magnetite nanocore for dilution-resistant biocompatible magnetic fluids*. Langmuir, 28(48), 16638–16646 (2012). DOI: [10.1021/la302660p](https://doi.org/10.1021/la302660p)
- 24 Fűredi-Milhofer H., Sarig S., *Interactions between polyelectrolytes and sparingly soluble salts*. Progress in Crystal Growth and Characterization of Materials, 32(1–3), 45–74 (1996). DOI: [10.1016/0960-8974\(96\)00006-X](https://doi.org/10.1016/0960-8974(96)00006-X)
- 25 Araujo P. Z., Morando P. J., Blesa M. A., *Interaction of catechol and gallic acid with titanium dioxide in aqueous suspensions. I. Equilibrium studies*. Langmuir, 21(8), 3470–3474 (2005). DOI: [10.1021/la0476985](https://doi.org/10.1021/la0476985)
- 26 Kearley G. J., Johnson M. R., Tomkinson J., *Intermolecular interactions in solid benzene*. The Journal of Chemical Physics, 124(4), 044514 (2006). DOI: [10.1063/1.2145926](https://doi.org/10.1063/1.2145926)
- 27 Tombácz E., Tóth I. Y., Nesztor D., Illés E., Hajdú A., Szekeres M., Vékás L., *Adsorption of organic acids on magnetite nanoparticles, pH-dependent colloidal stability and salt tolerance*. Colloids and Surfaces A: Physicochemical Engineering Aspects, 435, 91–96 (2013). DOI: [10.1016/j.colsurfa.2013.01.023](https://doi.org/10.1016/j.colsurfa.2013.01.023)
- 28 Borkovec M., Papastavrou G., *Interactions between solid surfaces with adsorbed polyelectrolytes of opposite charge*. Current Opinion in Colloid and Interface Science, 13(6), 429–437 (2008). DOI: [10.1016/j.cocis.2008.02.006](https://doi.org/10.1016/j.cocis.2008.02.006)
- 29 Hu J.-D., Zevi Y., Kou X.-M., Xiao J., Wang X.-J., Jin Y., *Effect of dissolved organic matter on the stability of magnetite nanoparticles under different pH and ionic strength conditions*. Science of The Total Environment, 408(16), 3477–3489 (2010). DOI: [10.1016/j.scitotenv.2010.03.033](https://doi.org/10.1016/j.scitotenv.2010.03.033)
- 30 Réthy B., Csupor-Löffler B., Zupkó I., Hajdú Zs., Imre M., Hohmann J., Rédei T., Falkay G., *Antiproliferative activity of Hungarian Asteraceae species against human cancer cell lines. Part I*. Phytotherapy Research, 21(12), 1200–1208 (2007). DOI: [10.1002/ptr.2240](https://doi.org/10.1002/ptr.2240)
- 31 Andreas K., Georgieva R., Ladwig M., Mueller S., Notter M., Sittinger M., Ringe J., *Highly efficient magnetic stem cell labeling with citrate-coated superparamagnetic iron oxide nanoparticles for MRI tracking*. Biomaterials, 33(18), 4515–4525 (2012). DOI: [10.1016/j.biomaterials.2012.02.064](https://doi.org/10.1016/j.biomaterials.2012.02.064)
- 32 Lévy M., Lagarde F., Maraloiu V. A., Blanchin M. G., Gendron F., Wilhelm C., Gazeau F., *Degradability of superparamagnetic nanoparticles in a model of intracellular environment: follow-up of magnetic, structural and chemical properties*. Nanotechnology, 21(39), 395103 (2010). DOI: [10.1088/0957-4484/21/39/395103](https://doi.org/10.1088/0957-4484/21/39/395103)
- 33 Taupitz M., Wagner S., Schnorr J., Kravec I., Pilgrim H., Bergmann-Fritsch H., Hamm B., *Phase I Clinical Evaluation of Citrate-coated Monocrystalline Very Small Superparamagnetic Iron Oxide Particles as a New Contrast Medium for Magnetic Resonance Imaging*. Investigative Radiology, 39(7), 394–405 (2004).